Int. J. Solids Structures Vol. 27, No. 10, pp. 1295–1309, 1991
Printed in Great Britain.

0020-7683/91 $3.00 + .00

THERMAL BUCKLING ANALYSIS OF ANTISYMMETRIC LAMINATED CYLINDRICAL SHELL PANELS

JENG-SHIAN CHANG and WEI-CHONG CHIU
Institute of Applied Mechanics, National Taiwan University, Taipei, Taiwan 10764, R.O.C.

(*Received* 12 *November* 1989; *in revised form* 19 *May* 1990)

Abstract—The thermal buckling analysis of antisymmetric angle-ply laminated cylindrical shells that are simply supported and subjected to a uniform temperature rise is analyzed by a finite element method based on the higher order displacement functions. Comparisons to the first order displacement theory are made. Both theories allow transverse shear deformation, but only the higher order one takes into account the transverse normal strain. The numerical results show that first order theory overestimates the thermal buckling temperature of the shell panel, which suggests that the higher order displacement fields should be used in the analysis of thermal buckling for a laminated shell. Effects of important parameters are also studied.

NOMENCLATURE

a, b	length of the cylindrical panel along x and θ directions, respectively
$[A], [B], [D], [F], [G], [L], [\Lambda]$	stiffness matrices of zero, first, $\cdots$, and sixth moments of the cylindrical panel, respectively
E_i, G_{ij}	Young's moduli and shear moduli, respectively
h	thickness of the cylindrical panel
$[K_g]$	geometrical stiffness matrix of the cylindrical panel
$[K_s]$	structural stiffness matrix of the cylindrical panel
N^T, M^T, R^T, S^T	thermal stress resultants of zero, first, second, and third moments, respectively
$Q_{ij}, \bar{Q}_{ij}$	stiffness of the lamina
R	radius of the cylindrical panel
$T(\bar{x}, \bar{y})$	temperature distribution
$[\ ]^t$	matrix transpose
U	strain energy
u, v, w	displacement functions along x–θ–z directions, respectively
u^0, v^0, w^0	displacement functions in the midplane
$u^*, v^*, w^*, \sigma^*, \varepsilon^*$	perturbation quantities to buckling configuration after the onset of buckling
$\alpha_1, \alpha_2, \alpha_3$	thermal expansion coefficients of the lamina along material principal directions
$\alpha_{xx}, \alpha_{yy}, \alpha_{zz}, \alpha_{xy}$	thermal expansion coefficients of the lamina under transformed coordinates x–y–z
$\varepsilon_x, \varepsilon_\theta, \varepsilon_z$	strains along x–θ–z directions, respectively
ε_{ij}	total strain components
$\varepsilon_{ij}^0, \{\varepsilon^0\}$	midplane strain components and vectors, respectively
$\{\Gamma\}, \{\beta\}, \{H\}$	generalized curvature vectors
$\psi_x, \psi_\theta, \psi_z$	generalized rotations
$\Delta T, \Delta T_{cr}, \Delta T_{cr}^*$	temperature rise, critical temperature rise and dimensionless critical temperature rise, respectively
θ	ply angle.

INTRODUCTION

Thermal buckling analysis is important in the design of thin shell structures in supersonic flight vehicles or other applications where the operating environment may undergo a temperature rise. Most of the existing papers deal only with mechanical in-plane load buckling, but a few discuss thermal buckling but for laminated plates. As for the thermal buckling problems of laminated shells the existing literature is rather meager. Hoff (1957) analyzed the thermal buckling of a simply supported thin cylindrical shell, Zuk (1957) investigated thermal buckling of clamped cylindrical shells using the Galerkin method, and Abir and Nardo (1959), Hoff *et al.* (1964) and Ross *et al.* (1965, 1966) discussed similar problems under different temperature environments. All of them are limited to isotropic materials. However, Gupta and Wang (1973) and Radhamohan and Venkataramana (1975) discussed thermal buckling of orthotropic shells with the effects of transverse thermal expansion neglected.

Zukas (1974) pointed out in the analysis of thermal deformation of laminates consisting of pyrolytic graphite possessing a high ratio of transverse to in-plane thermal expansion coefficients (α_{33}/α_{11}) that the effect of transverse shear and normal strains should not be neglected. In this paper we hence adopt a higher order displacement theory for the thermal analysis of laminated cylindrical shell panels. With the higher order terms of displacements along both the in-plane and the thickness direction, the transverse shear and the transverse normal deformations are all allowed. Effects of the ratio of transverse to in-plane thermal expansion coefficients are studied, and comparisons between the present high order theory and Mindlin–Reissner first order theory are made. Other interesting parameters affecting the critical temperatures, such as ply angle, ratio of transverse to in-plane moduli, number of layers, boundary support conditions, etc., are also investigated, and the results are presented in this paper.

GOVERNING EQUATIONS

Displacement fields

Referring to Fig. A(a), consider a cylindrical shell panel with radius R, thickness h, longitudinal span a, and circumferential span b. In order to take into account the transverse shear and normal deformations, the following displacement field is assumed in the sequel:

$$
\begin{aligned}
u &= u^0(x,\theta) + z\psi_x(x,\theta) + z^3\xi_x(x,\theta)\\
v &= v^0(x,\theta) + z\psi_\theta(x,\theta) + z^3\xi_\theta(x,\theta)\\
w &= w^0(x,\theta) + z\psi_z(x,\theta) + z^2\eta_z(x,\theta).
\end{aligned} \tag{1}
$$

Unlike the first order Mindlin-type displacement field, the above displacement field avoids the use of a shear correction factor.

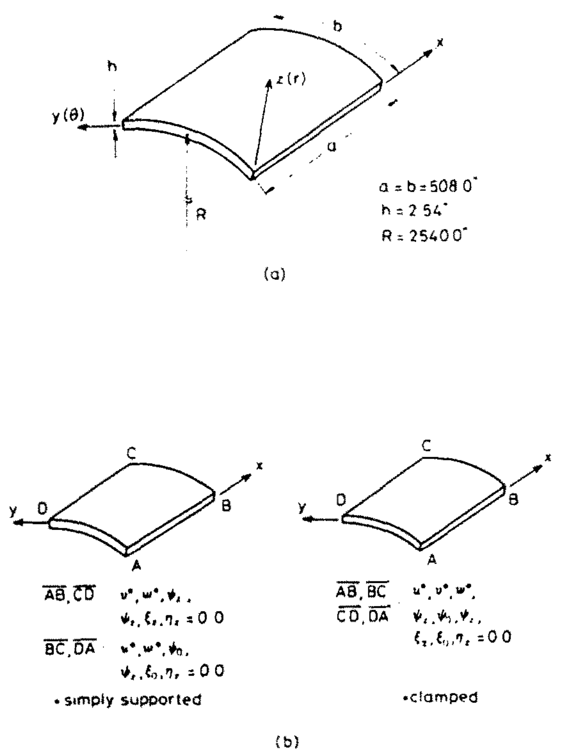

Fig. A. Geometrical configuration (a) and boundary support conditions (b) of the laminated cylindrical shell panel. $E_1/E_0 = 21.0$, $E_2/E_0 = 1.7$, $E_3 = E_2$, $G_{12}/E_0 = 0.65$, $G_{23}/E_0 = 0.639$, $G_{13} = G_{12}$, $\nu_{12} = \nu_{13} = 0.21$, $\nu_{23} = 0.33$, $\alpha_{11} = -0.21$, $\alpha_{22}/\alpha_0 = \alpha_{33}/\alpha_0 = 16.0$, $E_0 = 1 \times 10^6$ psi, $\alpha_0 = 1 \times 10^{-6}$ in/in/°F.

Strain–displacement relationships

Since buckling is a nonlinear phenomenon, the geometrically nonlinear strain–displacement relationship is required to derive the associated governing equation. Such nonlinear strain–displacement relations for the cylindrical shells were provided by Novozhilov (1953), and read:

$$
\begin{aligned}
\varepsilon_x &= \{(1+u_{,x})^2+(v_{,x})^2+(w_{,x})^2\}^{1/2}-1 \\
\varepsilon_\theta &= \{(u_{,\theta}/r)^2+(1+v_{,\theta}/r+w/r)^2+(w_{,\theta}/r-v/r)^2\}^{1/2}-1 \\
\varepsilon_r &= \{(u_{,r})^2+(v_{,r})^2+(1+w_{,r})^2\}^{1/2}-1 \\
\gamma_{x\theta} &= \{(1+u_{,x})(u_{,\theta}/r)+v_{,x}(1+v_{,\theta}/r+w/r)+(w_{,x})(w_{,\theta}/r-v/r)\}/ \\
&\quad \{[(1+u_{,x})^2+(v_{,x})^2+(w_{,x})^2]^{1/2}[(u_{,\theta}/r)^2+(1+v_{,\theta}/r+w/r)^2+(w_{,\theta}/r-v/r)^2]^{1/2}\} \\
\gamma_{xr} &= \{(1+u_{,x})(u_{,r})+(v_{,x})(v_{,r})+(w_{,x})(1+w_{,r})\}/\{[(1+u_{,x})^2+(v_{,x})^2+(w_{,x})^2]^{1/2} \\
&\quad \times[(u_{,r})^2+(v_{,r})^2+(1+w_{,r})^2]^{1/2}\} \\
\gamma_{\theta r} &= \{(u_{,r})(u_{,\theta}/r)+(1+v_{,\theta}/r+w/r)(v_{,r})+(1+w_{,r})(w_{,\theta}/r-v/r)\}/ \\
&\quad \{[(u_{,r})^2+(v_{,r})^2+(1+w_{,r})^2]^{1/2}[(u_{,\theta}/r)^2+(1+v_{,\theta}/r+w_{,r})^2+(w_{,\theta}/r-v/r)^2]^{1/2}\}. \qquad (2)
\end{aligned}
$$

We then expand the above relations, drop terms with order higher than two, and neglect part of the second order terms but reserve some appropriate ones by comparing their order of magnitude as Stein (1986) did. For example, in the first relation of the above equation, the second order term $(u_{,x})^2/2$ can be neglected due to the existence of $u_{,x}$ but the terms $(v_{,x})^2/2$ and $(w_{,x})^2/2$ cannot. Then the above nonlinear strain-displacement relations reduce to the following:

$$
\begin{aligned}
\varepsilon_x &= u_{,x}+(v_{,x})^2/2+(w_{,x})^2/2 \\
\varepsilon_\theta &= (u_{,\theta}/r)^2/2+(v_{,\theta}+w)/r+(w_{,\theta}/r-v/r)^2 \\
\varepsilon_r &= (u_{,r})^2/2+(v_{,r})^2/2+w_{,r} \\
\gamma_{x\theta} &= (u_{,\theta}/r)(1-v_{,\theta}-w/r)+(w_{,x})(w_{,\theta}/r+v/r)+(v_{,x})(1-u_{,x}) \\
\gamma_{xr} &= (1-w_{,r})(u_{,r})+(v_{,x})(v_{,r})+(w_{,x})(1-u_{,x}) \\
\gamma_{\theta r} &= (u_{,\theta}/r)(u_{,r})+(1-v_{,\theta}/r-w/r)(w_{,\theta}/r-v/r)+(v_{,r})(1-w_{,r}). \qquad (3)
\end{aligned}
$$

Substituting the displacement field, eqn (1), into the above equations, neglecting terms of higher order product of z than 4 inclusive, and keeping the products of the larger rotational quantities, $w^0_{,x}$ and $(w^0_{,\theta}-v^0)/r$, yields

$$
\begin{aligned}
\varepsilon_x &= u^0_{,x}+z\psi_{x,x}+z^3\xi_{x,x}+(w^0_{,x})^2/2 \\
\varepsilon_\theta &= \frac{v^0_{,\theta}}{r}+\frac{z}{r}\psi_{\theta,\theta}+\frac{z^3}{r}\xi_{\theta,\theta}+\frac{w^0}{r}+\frac{z}{r}\psi_z+\frac{z^2}{r}\eta_z+\frac{(w^0_{,\theta}-v^0)^2}{2r^2} \\
\varepsilon_r &= \psi_z+2z\eta_z \\
\gamma_{\theta r} &= \frac{w^0_{,\theta}}{r}+\frac{z}{r}\psi_{z,\theta}+\frac{z^2}{r}\eta_{z,\theta}-\frac{v^0}{r}-\frac{z}{r}\psi_\theta-\frac{z^3}{r}\xi_\theta+\psi_\theta+3z^2\xi_\theta \\
\gamma_{xr} &= \psi_z+3z^2\xi_x+w^0_{,x}+z\psi_{z,x}+z^2\eta_{z,x} \\
\gamma_{x\theta} &= \frac{1}{r}u^0_{,\theta}+\frac{z}{r}\psi_{z,\theta}+\frac{z^3}{r}\xi_{x,\theta}+v^0_{,x}+z\psi_{\theta,x}+z^3\xi_{\theta,x}+\frac{w^0_{,\theta}}{r}w^0_{,x}-\frac{v^0}{r}w^0_{,x}. \qquad (4)
\end{aligned}
$$

In this study, only $R \gg z$ is considered. Under this assumption,

$$r = R + z \approx R$$

$$\mathrm{d}y = R\,\mathrm{d}\theta.$$

Thus, one can replace the (x, θ, r) coordinates by (x, y, z) coordinates, and since R is a constant, then

$$\mathrm{d}x = \mathrm{d}x$$

$$\mathrm{d}\theta = \frac{\mathrm{d}y}{R}$$

$$\mathrm{d}r = \mathrm{d}z.$$

In the following, the (x, y, z) system will be used. Under such a system and the assumption $R \gg z$, eqn (4) is simplified and revised to read as

$$\{\varepsilon\} = \{\varepsilon^0\} + z\{\Gamma\} + z^2\{\beta\} + z^3\{H\} \tag{5}$$

where

$$\varepsilon_x^0 = u_{,x}^0 + \tfrac{1}{2}(w_{,x}^0)^2$$

$$\varepsilon_y^0 = v_{,y}^0 + \frac{w^0}{R} + \frac{1}{2}\left(w_{,y}^0 - \frac{v^0}{R}\right)^2$$

$$\varepsilon_z^0 = \psi_z$$

$$\gamma_{yz}^0 = w_{,y}^0 - \frac{v^0}{R} + \psi_\theta$$

$$\gamma_{xz}^0 = \psi_x + w_{,x}^0$$

$$\gamma_{xy}^0 = u_{,y}^0 + v_{,x}^0 + w_{,x}^0 w_{,y}^0 - \frac{v^0}{R} w_{,x}^0$$

$$\Gamma_x = \psi_{x,x}$$

$$\Gamma_y = \psi_{\theta,y} + \frac{\psi_z}{R}$$

$$\Gamma_z = 2\eta_z$$

$$\Gamma_{yz} = \psi_{z,y} - \frac{\psi_\theta}{R}$$

$$\Gamma_{xz} = \psi_{z,x}$$

$$\Gamma_{xy} = \psi_{x,y} + \psi_{\theta,x}$$

$$\beta_x = \beta_z = \beta_{xy} = 0$$

$$\beta_y = \frac{\eta_z}{R}$$

$$\beta_{yz} = \eta_{z,y} + 3\xi_\theta$$

$$\beta_{xz} = \eta_{z,x} + 3\xi_x$$

$$H_x = \xi_{x,x}$$

$$H_y = \xi_{\theta,y}$$

$$H_z = H_{xz} = 0$$

$$H_{yz} = -\frac{\xi_\theta}{R}$$

$$H_{xy} = \xi_{x,y} + \xi_{\theta,x}. \tag{6}$$

Stress–strain relationships

The stress–strain relations for a unidirectional lamina in its principal material directions 1-2-3 are:

$$\begin{bmatrix} \sigma_{11} \\ \sigma_{22} \\ \sigma_{33} \\ \sigma_{23} \\ \sigma_{31} \\ \sigma_{12} \end{bmatrix} = \begin{bmatrix} Q_{11} & Q_{12} & Q_{13} & 0 & 0 & 0 \\ Q_{12} & Q_{22} & Q_{23} & 0 & 0 & 0 \\ Q_{13} & Q_{23} & Q_{33} & 0 & 0 & 0 \\ 0 & 0 & 0 & Q_{44} & 0 & 0 \\ 0 & 0 & 0 & 0 & Q_{55} & 0 \\ 0 & 0 & 0 & 0 & 0 & Q_{66} \end{bmatrix} \begin{Bmatrix} \varepsilon_{11} - \alpha_1 \Delta T \\ \varepsilon_{22} - \alpha_2 \Delta T \\ \varepsilon_{33} - \alpha_3 \Delta T \\ \gamma_{32} \\ \gamma_{13} \\ \gamma_{12} \end{Bmatrix}. \tag{7}$$

Referring to the x–y–z coordinates, the above equations can be transformed into

$$\begin{bmatrix} \sigma_x \\ \sigma_y \\ \sigma_z \\ \sigma_{yz} \\ \sigma_{xz} \\ \sigma_{xy} \end{bmatrix} = \begin{bmatrix} \bar{Q}_{11} & \bar{Q}_{12} & \bar{Q}_{13} & 0 & 0 & \bar{Q}_{16} \\ \bar{Q}_{12} & \bar{Q}_{22} & \bar{Q}_{23} & 0 & 0 & \bar{Q}_{26} \\ \bar{Q}_{13} & \bar{Q}_{23} & \bar{Q}_{33} & 0 & 0 & \bar{Q}_{36} \\ 0 & 0 & 0 & \bar{Q}_{44} & \bar{Q}_{45} & 0 \\ 0 & 0 & 0 & \bar{Q}_{54} & \bar{Q}_{55} & 0 \\ \bar{Q}_{16} & \bar{Q}_{26} & \bar{Q}_{36} & 0 & 0 & \bar{Q}_{66} \end{bmatrix} \begin{Bmatrix} \varepsilon_x - \alpha_{xx} \Delta T \\ \varepsilon_y - \alpha_{yy} \Delta T \\ \varepsilon_z - \alpha_{zz} \Delta T \\ \gamma_{yz} \\ \gamma_{xz} \\ \gamma_{xy} - 2\alpha_{xy} \Delta T \end{Bmatrix}. \tag{8}$$

$$= [\bar{Q}](\{\varepsilon\} - \{\alpha\}\Delta T)$$

The transformation between eqns (7) and (8) can be found in standard textbooks, such as Vinson and Sierakowski (1986).

Total potential energy

The total potential energy π is equal to the difference of total strain energy U and the external work W. In the thermal buckling problem, there is no external work W. So $\pi = U$, and U is given as

$$U = \int_V \tfrac{1}{2}(\sigma_{xx}\bar{\varepsilon}_{xx} + \sigma_{yy}\bar{\varepsilon}_{yy} + \sigma_{zz}\bar{\varepsilon}_{zz} + \sigma_{yz}\bar{\gamma}_{yz} + \sigma_{xz}\bar{\gamma}_{xz} + \sigma_{xy}\bar{\gamma}_{xy})\, \mathrm{d}V \tag{9}$$

where

$$\bar{\varepsilon}_{ij} = \varepsilon_{ij} - \alpha_{ij}\Delta T,$$

$$\varepsilon_{ij} = \text{total strain},$$

$$\alpha_{ij}\Delta T = \text{thermal strain}.$$

Substituting eqn (8) into the above equation yields

$$U = \sum_{k=1}^{n} U_k = \sum_{k=1}^{n} \frac{1}{2} \int_{V_k} (\{\varepsilon\} - \{\alpha\}\Delta T)_k^t \{\sigma\}_k \, \mathrm{d}V_k$$

$$= \sum_{k=1}^{n} \frac{1}{2} \int_{V_k} (\{\varepsilon\} - \{\alpha\}\Delta T)_k^t [\bar{Q}]_k (\{\varepsilon\} - \{\alpha\}\Delta T)_k \, \mathrm{d}V_k \tag{10}$$

where subscript k denotes the kth layers of the laminated shell and n is the total number of the layers. Substituting eqn (5) into eqn (10) and then integrating through thickness h yields

$$U = \frac{1}{2}\int_{\Omega} \{\varepsilon^0\}^t\{\Gamma\}^t\{\beta\}^t\{H\}^t \begin{bmatrix} A & B & D & F \\ B & D & F & G \\ D & F & G & L \\ F & G & L & \Lambda \end{bmatrix} \begin{Bmatrix} \{\varepsilon^0\} \\ \{\Gamma\} \\ \{\beta\} \\ \{H\} \end{Bmatrix} \mathrm{d}\Omega$$

$$- \int_{\Omega} \{\varepsilon^0\}^t\{\Gamma\}^t\{\beta\}^t\{H\}^t \begin{Bmatrix} \{N^T\} \\ \{M^T\} \\ \{R^T\} \\ \{S^T\} \end{Bmatrix} \mathrm{d}\Omega \quad (11)$$

where Ω is the area of the middle plane of the shell and

$$(A_{ij}, B_{ij}, D_{ij}) = \sum_{k=1}^{n} \int_{z_{k-1}}^{z_k} (1, z, z^2)(\bar{Q}_{ij})_k \, \mathrm{d}z$$

$$(F_{ij}, G_{ij}, L_{ij}, \Lambda_{ij}) = \sum_{k=1}^{n} \int_{z_{k-1}}^{z_k} (z^3, z^4, z^5, z^6)(\bar{Q}_{ij})_k \, \mathrm{d}z$$

$$(\{N^T\}\{M^T\}\{R^T\}\{S^T\}) = \sum_{k=1}^{n} \int_{z_{k-1}}^{z_k} [\bar{Q}_{ij}]_k \{\alpha\}_k (1, z, z^2, z^3)\Delta T \, \mathrm{d}z \quad (12)$$

and z_k, z_{k-1} denote the z coordinates of the upper and lower surfaces of the kth layer, respectively.

Thermal stress analysis

The thermal stresses and deformation before buckling can be analyzed by using the principle of stationary total potential energy. Taking the first variation of the strain energy U produces

$$0 = \delta U = \int_V (\sigma_{xx}\delta\varepsilon_{xx} + \sigma_{yy}\delta\varepsilon_{yy} + \sigma_{zz}\delta\varepsilon_{zz} + \sigma_{yz}\delta\gamma_{yz} + \sigma_{xz}\delta\gamma_{xz} + \sigma_{xy}\delta\gamma_{xy}) \, \mathrm{d}V. \quad (13)$$

Substituting eqn (5) into the above equation and integrating through the thickness yields

$$0 = \delta U = \frac{1}{2}\int_{\Omega} (\{\delta\varepsilon^0\}^t\{\delta\Gamma\}^t\{\delta\beta\}^t\{\delta H\}^t)[C] \begin{bmatrix} A & B & D & F \\ B & D & F & G \\ D & F & G & L \\ F & G & L & \Lambda \end{bmatrix} \begin{Bmatrix} \varepsilon^0 \\ \Gamma \\ \beta \\ H \end{Bmatrix} \mathrm{d}\Omega$$

$$- \int_{\Omega} (\{\delta\varepsilon^0\}^t\{\delta\Gamma\}^t\{\delta\beta\}^t\{\delta H\}^t) \begin{Bmatrix} N^T \\ M^T \\ R^T \\ S^T \end{Bmatrix} \mathrm{d}\Omega \quad (14)$$

where

$$[C] = \begin{bmatrix} A & B & D & F \\ B & D & F & G \\ D & F & G & L \\ F & G & L & \Lambda \end{bmatrix}. \quad (15)$$

Discretizing eqn (14), and using the appropriate shape functions $[\Phi]$ to denote

$$\begin{aligned}\{\varepsilon^0\}_e &= [\Phi_{\varepsilon^0}]\{d_{\varepsilon^0}\}_e \\ \{\Gamma\}_e &= [\Phi_\Gamma]\{d_\Gamma\}_e \\ \{\beta\}_e &= [\Phi_\beta]\{d_\beta\}_e \\ \{H\}_e &= [\Phi_H]\{d_H\}_e\end{aligned} \tag{16}$$

where $\{d_{\varepsilon^0}\}_e, \ldots$ are element nodal displacements, one then obtains

$$\begin{aligned}\delta U &= \sum_{e=1}^{N_e} \delta U^{(e)} \\ &= \{\delta d\}^t \left(\sum_{e=1}^{N_e} \int_{\Omega_e} ([\Phi_{\varepsilon^0}]^t [\Phi_\Gamma]^t [\Phi_\beta]^t [\Phi_H]^t)[C] \begin{Bmatrix} [\Phi_{\varepsilon^0}] \\ [\Phi_\Gamma] \\ [\Phi_\beta] \\ [\Phi_H] \end{Bmatrix} \mathrm{d}\Omega_e \right) \{d\} \\ &\quad - \{\delta d\}^t \left(\sum_{e=1}^{N_e} \int_{\Omega_e} ([\Phi_{\varepsilon^0}]^t [\Phi_\Gamma]^t [\Phi_\beta]^t [\Phi_H]^t) \begin{Bmatrix} \{N^T\} \\ \{M^T\} \\ \{R^T\} \\ \{S^T\} \end{Bmatrix} \mathrm{d}\Omega_e \right) \\ &= \{\delta d\}^t([K_s]\{d\} - \{P\})\end{aligned} \tag{17}$$

where

N_e = total number of elements discretized

$U^{(e)}$ = strain energy of a single element

superscript t denotes the matrix transpose.

Equating eqn (17) to zero, the following matrix equation is obtained:

$$[K_s]\{d\} = \{P\} \tag{18}$$

where

$[K_s] = \sum [K_s]_e$ = stiffness matrix of the whole structure

$[K_s]_e$ = stiffness matrix of a single element

$$\{d\} = \sum \{d\}_e = \sum \begin{Bmatrix} \{d_{\varepsilon^0}\}_e \\ \{d_\Gamma\}_e \\ \{d_\beta\}_e \\ \{d_H\}_e \end{Bmatrix}$$

= displacement vector of the nodal points of the system

$\{P\} = \sum \{P\}_e$ = load vector.

Thermal buckling equations

According to the Euler method shown by Washizu (1986) or the adjacent equilibrium method depicted by Brush and Almroth (1975), we add an infinitesimal perturbation along the bifurcation path to the equilibrium state at the bifurcation point due to thermal buckling. Thus, we denote the original state and the bifurcated state as

$$\sigma_{ij}, e_{ij}, u_{ij}$$

and

$$\sigma_{ij}+\sigma^*_{ij}, e_{ij}+e^*_{ij}, u_{ij}+u^*_{ij}, \text{ respectively,}$$

where σ^*_{ij}, e^*_{ij}, u^*_i are infinitesimal increments, and

$$2(e_{ij}+e^*_{ij}) = (u_i+u^*_i)_{,j}+(u_j+u^*_j)_{,i}+(u_k+u^*_k)_{,i}(u_k+u^*_k)_{,j}. \tag{19}$$

Applying the principle of stationary total potential energy again:

$$\delta(U+U^*) = \int_V (\sigma_{ij}+\sigma^*_{ij})\delta(e_{ij}+e^*_{ij})\,\mathrm{d}V = 0. \tag{20}$$

Noticing that $\delta U = 0$, the above equation can be reduced to the following form by neglecting the higher order terms of u^*_i:

$$\int_V (\sigma^*_{ij}\delta\varepsilon^*_{ij}+\sigma_{ij}u^*_{k,i})\,\mathrm{d}V = 0 \tag{21}$$

where

$$2\varepsilon^*_{ij} = u^*_{i,j}+u^*_{j,i}+u_{k,i}u^*_{k,j}+u^*_{k,i}u_{k,j}. \tag{22}$$

Equation (21) is the second variation of the total potential energy and represents the general form of bifurcation equation. In the case of the current cylindrical shell panel, the components of eqn (22) are given as follows:

$$\varepsilon^*_{xx} = u^*_{,x}+v_{,x}v^*_{,x}+w_{,x}w^*_{,x}$$

$$\varepsilon^*_{yy} = v^*_{,y}+\frac{w^*}{R}+u_{,y}u^*_{,y}+w_{,y}w^*_{,y}-\frac{v}{R}w^*_{,y}-\frac{v^*}{R}w_{,y}$$

$$\varepsilon^*_{zz} = w^*_{,z}+u_{,z}u^*_{,z}+v_{,z}v^*_{,z}$$

$$\gamma^*_{yz} = v^*_{,z}+w^*_{,y}-\frac{v^*}{R}+u_{,y}u^*_{,z}+u^*_{,y}u_{,z}-v_{,z}w^*_{,z}-v^*_{,z}w_{,z}-v_{,y}w^*_{,y}-v^*_{,y}w_{,y}+\frac{v^*}{R}v_{,y}$$
$$+\frac{v}{R}v^*_{,y}-\frac{w}{R}w^*_{,y}-\frac{w^*}{R}w_{,y}$$

$$\gamma^*_{xz} = u^*_{,z}+w^*_{,x}-u_{,z}w^*_{,z}-u^*_{,z}w_{,x}-u_{,x}w^*_{,x}-u^*_{,x}w_{,x}+v_{,x}v^*_{,z}+v^*_{,x}v_{,z}$$

$$\gamma^*_{xy} = u^*_{,y}+v^*_{,x}-u_{,y}v^*_{,y}-u^*_{,y}v_{,y}-u_{,y}\frac{w^*}{R}-u^*_{,y}\frac{w}{R}+w_{,x}w^*_{,y}+w^*_{,x}w_{,y}-w_{,x}\frac{v^*}{R}-w^*_{,x}\frac{v}{R}. \tag{23}$$

As pointed out by Brush and Almroth (1975), the product terms in the above equation can be neglected since the prebuckling strains are usually much smaller than unity, this eqn (23) can be simplified as

$$
\begin{aligned}
\varepsilon^*_{xx} &= u^*_{,x} \\
\varepsilon^*_{yy} &= v^*_{,y} + \frac{w^*}{R} \\
\varepsilon^*_{zz} &= w^*_{,z} \\
\gamma^*_{yz} &= v^*_{,z} + w^*_{,y} - \frac{v^*}{R} \\
\gamma^*_{xz} &= u^*_{,z} + w^*_{,x} \\
\gamma^*_{xy} &= u^*_{,y} + v^*_{,x}.
\end{aligned} \tag{24}
$$

Combining eqns (1) and (24), then substituting into eqn (21), and integrating through the thickness h, one obtains the following equation:

$$
\delta U^* = \int_\Omega (\{\delta\varepsilon^{0*}\}^t\{\delta\Gamma^*\}^t\{\delta\beta^*\}^t\{\delta H^*\}^t)[C]\begin{Bmatrix}\{\varepsilon^{0*}\}\\ \{\Gamma^*\}\\ \{\beta^*\}\\ \{H^*\}\end{Bmatrix}\mathrm{d}\Omega
$$

$$
+\int_\Omega \begin{pmatrix}\delta w^{0*}_{,x}\\ \delta\left(w^{0*}_{,y} - \dfrac{v^{0*}}{R}\right)\end{pmatrix}\begin{bmatrix}\bar{N}_x & \bar{N}_{xy}\\ \bar{N}_{xy} & \bar{N}_y\end{bmatrix}\begin{Bmatrix}w^{0*}_{,x}\\ w^{0*}_{,y} - \dfrac{v^{0*}}{R}\end{Bmatrix}\mathrm{d}\Omega = 0. \tag{25}
$$

In the above equation, $\bar{N}_x$, $\bar{N}_y$, $\bar{N}_{xy}$ are the thermal stress resultants right before the onset of the buckling and are defined as:

$$
\begin{Bmatrix}\bar{N}_x\\ \bar{N}_y\\ \bar{N}_{xy}\end{Bmatrix} = \int_{-h/2}^{h/2}\begin{Bmatrix}\sigma_x\\ \sigma_y\\ \tau_{xy}\end{Bmatrix}\mathrm{d}z = \int_{-h/2}^{h/2}\begin{bmatrix}\bar{Q}_{11} & \bar{Q}_{12} & \bar{Q}_{16} & \bar{Q}_{13}\\ \bar{Q}_{12} & \bar{Q}_{22} & \bar{Q}_{26} & \bar{Q}_{23}\\ \bar{Q}_{16} & \bar{Q}_{26} & \bar{Q}_{66} & \bar{Q}_{36}\end{bmatrix}
$$

$$
\times\begin{Bmatrix}\varepsilon_x - \alpha_x\Delta T\\ \varepsilon_y - \alpha_y\Delta T\\ \gamma_{xy} - 2\alpha_{xy}\Delta T\\ \varepsilon_z - \alpha_z\Delta T\end{Bmatrix}\mathrm{d}z \tag{26}
$$

where ε_x, ε_y, γ_{xy}, and ε_z are the prebuckling strains, calculated based on the prebuckling deformation found from eqn (18). Discretizing eqn (25) yields the following characteristic equation:

$$
([K_s] + \Delta T[K_G])\{\bar{d}\} = 0 \tag{27}
$$

where

$$
[K_G] = \int_\Omega [\bar{G}]^T\begin{bmatrix}\bar{N}^0_x & \bar{N}^0_{xy}\\ \bar{N}^0_{xy} & \bar{N}^0_y\end{bmatrix}[\bar{G}]\,\mathrm{d}\Omega \tag{28}
$$

$$
\begin{Bmatrix}\bar{N}^0_x\\ \bar{N}^0_y\\ \bar{N}^0_{xy}\end{Bmatrix} = \frac{1}{\Delta T}\begin{Bmatrix}\bar{N}_x\\ \bar{N}_y\\ \bar{N}_{xy}\end{Bmatrix} \tag{29}
$$

and

$$\begin{Bmatrix} w^{(1)}_{,x} \\ w^{(1)}_{,y} - \dfrac{v^*}{R} \end{Bmatrix} = [\bar{G}]\{\bar{d}\}. \tag{30}$$

Solution of eqn (27) gives the thermal buckling temperature ΔT_{cr} and the corresponding mode shape $\{\bar{d}\}$. In this study, a nine-node isoparametric element is adopted.

NUMERICAL EXAMPLES

Refer to Fig. A(b), where two sets of boundary conditions, simply supported and clamped, are shown, and the shell panel is laminated as anti-symmetric angle-ply whose geometrical configuration, as already shown in Fig. A(a), and the material constants of each ply are given as follows:

$$\begin{aligned}
&[+\theta/-\theta/+\theta/-\theta/\cdots] \\
&\theta = \text{ply angle} \\
&a = \text{edge length} \\
&h = \text{thickness} \\
&E_1/E_0 = 21, \quad E_0 = 10^6 \text{ psi} \\
&E_2/E_0 = 1.7, \quad E_3/E_0 = 1.7 \\
&G_{12}/E_0 = 1.7, \quad G_{13}/E_0 = 0.65 \\
&G_{23}/E_0 = 0.639 \\
&\nu_{12} = \nu_{13} = 0.21 \\
&\nu_{23} = 0.33 \\
&\alpha_1 = -0.21 \times 10^{-6} \text{ in/in/}^\circ\text{F} \\
&\alpha_2 = \alpha_3 = \alpha_0 = 10^{-6} \text{ in/in/}^\circ\text{F}.
\end{aligned} \tag{31}$$

The above material constants will be applied to each numerical example in the following except that part of the material constants will be altered to investigate the sensitivity of these moduli on the thermal buckling temperature and this will be pointed out at the appropriate place. Numerical solutions of thermal buckling temperature, with the unit °F, are given in Tables 1 and 2 and Figs 1–8, which will be discussed below.

(1) Effect of transverse thermal expansion coefficient: *referring to Table 1, comparisons of the thermal buckling temperature by varying the ratios of α_3 to α_1 between the current theory using displacement field, eqn (1), and the Mindlin–Reissner first order displacement theory, the special case of eqn (1) without higher order terms of z than one, are made. As can be observed in this table, the difference of buckling temperature predicted by the two theories increases as the ratio of α_3 to α_1 increases. Also, the discrepancy is bigger in the case of two layers than six layers, which may be contributed to the larger bending-extension coupling of the former than the latter. Thus it may be concluded that in the case of a large transverse thermal expansion coefficient compared to the in-plane thermal expansion coefficient in the fiber direction, a higher order displacement field should be used to obtain more accurate results.

(2) Effect of ply angle: Fig. 1a,b presents the relationships of the critical temperature of thermal buckling versus ply angle θ for the shell panel with layers 2, 4, and 6 under simply-supported and clamped boundary conditions, respectively. As they show, the critical temperature rises rapidly when the ply angle reaches 35° and obtains its maximum at about 40°, and then drops drastically when the ply angle is greater than 45°. Additionally, there is a local maximum and minimum near ply angles 10° and 23°, respectively, in the case of simply-supported boundary and layers 4 and 6. Table 2 then lists the ply angles where the

Table 1. Comparisons of present and Mindlin theory for ΔT_{cr} (°F) for a six-layer simply-supported laminated shell panel, $[-45°/45°]_3$, with $a/h = 200$, $a/b = 1$, $E_1/E_0 = 21$, $E_2/E_0 = 1.7$, $E_3 = E_2$, $G_{12}/E_0 = 0.65$, $G_{23}/E_0 = 0.639$, $G_{13} = G_{12}$, $\nu_{12} = \nu_{13} = 0.21$, $\nu_{23} = 0.33$, $\alpha_1 = -0.21$, $\alpha_2/\alpha_0 = \alpha_3/\alpha_0 = 16.0$, $E_0 = 1 \times 10^6$ psi, $\alpha_0 = 1 \times 10^{-6}$ in/in/°F

No. of layers	α_3/α_1	Critical temp. (A) (Mindlin)	Critical temp. (B) (Present)	Difference (A-B)/B (%)
2	1.00	576.24	547.10	5.32
	5.00	427.00	389.37	9.66
	10.00	322.66	286.26	12.72
	20.00	217.21	187.30	15.97
	30.00	163.90	139.43	17.55
	40.00	131.82	111.17	18.57
	50.00	110.31	92.59	19.14
	75.00	78.66	65.49	20.13
	100.00	61.33	50.88	20.54
6	1.00	768.11	762.11	0.79
	5.00	568.87	547.85	3.84
	10.00	429.79	405.37	6.02
	20.00	288.96	266.88	8.27
	30.00	217.88	199.13	9.41
	40.00	175.01	159.02	10.06
	50.00	146.35	132.43	10.51
	75.00	104.06	132.43	11.14
	100.00	80.94	72.62	11.45

Table 2. Ply angles corresponding to maximum critical temperatures for various numbers of layers and boundary supported conditions, antisymmetric angle-ply laminated shell panel, $[(+\theta/-\theta/\cdots)]$, $a/h = 200$, $a/b = 1$, $E_1/E_0 = 21$, $E_2/E_0 = 1.7$, $E_3 = E_2$, $G_{12}/E_0 = 0.65$, $G_{23}/E_0 = 0.639$, $G_{13} = G_{12}$, $\nu_{12} = \nu_{13} = 0.21$, $\nu_{23} = 0.33$, $\alpha_1 = -0.21$, $\alpha_2/\alpha_0 = \alpha_3/\alpha_0 = 16.0$, $E_0 = 10^6$ psi, $\alpha_0 = 10^{-6}$ in/in/°F

No. of layers	Simply-supported Angle	Simply-supported ΔT^*_{cr}	Clamped Angle	Clamped ΔT^*_{cr}
2	41.5°	794.42	42.5°	616.59
4	41.5°	989.12	42.5°	803.76
6	41.5°	1014.84	42.5°	831.88

maximum critical temperatures occur for the simply supported and clamped boundary conditions as well as various number of layers, respectively.

(3) Effect of modulus ratio of E_1 to E_2: Fig. 2a,b depicts the effect of E_1/E_2. As can be seen, the critical temperatures for various numbers of layers come closer and closer as the ratio of E_1/E_2 varies from large to unity, which means that the bending-extension

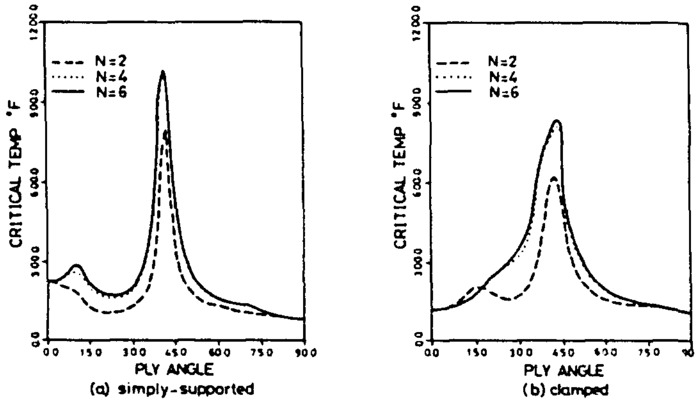

Fig. 1. Effect of ply angle on critical temperature of thermal buckling. (a) Simply-supported. (b) Clamped.

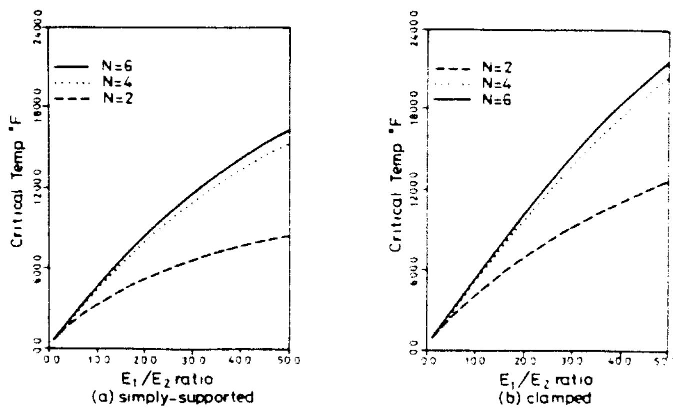

Fig. 2. Effect of modulus ratio E_1/E_2 on critical temperature of thermal buckling. (a) Simply-supported. (b) Clamped. $E_2/E_0 = 1.7$, $E_3 = E_2$, $G_{12}/E_0 = 0.65$, $G_{23}/E_0 = 0.639$, $G_{13} = G_{12}$, $\nu_{12} = \nu_{13} = 0.21$, $\nu_{23} = 0.33$, $\alpha_{11} = -0.21$, $\alpha_{22}/\alpha_0 = \alpha_{33}/\alpha_0 = 16.0$, $E_0 = 1 \times 10^6$ psi, $\alpha_0 = 1 \times 10^{-6}$ in/in/°F.

coupling is also getting smaller. Since in the case of a two-layer panel, the effect of bending–extension is the largest, therefore its critical temperature is smaller than those of four-layer and six-layer panels with the thickness unchanged.

(4) Effect of radius of curvature: Fig. 3a,b shows the effect of the ratio of thickness h to radius of curvature R. As illustrated in the figure, the larger the value of h/R, the higher the critical temperature, which means the larger curvature may stabilize the structure, as expected.

(5) Effect of span ratio a/b: Fig. 4a,b presents the relationships of the critical temperature versus span ratio a/b. As observed, the critical temperature reaches a maximum and then drop as a/b varies from small to large. The ripples in the curves of the figures are attributed to the change of buckling modes, which are illustrated in Figs 5a–f and 6a–f. By comparing Figs 5 and 6 it can be concluded that more mode jumping occurs in the case of a simply-supported boundary than a clamped boundary.

(6) Effect of boundary conditions: Fig. 7 compares the effect of different boundary conditions on the critical temperature under various values of h/R. Although a clamped boundary usually stiffens the panel, and hence increases the critical temperature of thermal buckling, in contrast to the simply-supported panel at the same level of temperature, the same boundary condition also raises the thermal stresses in the panel, which tends to

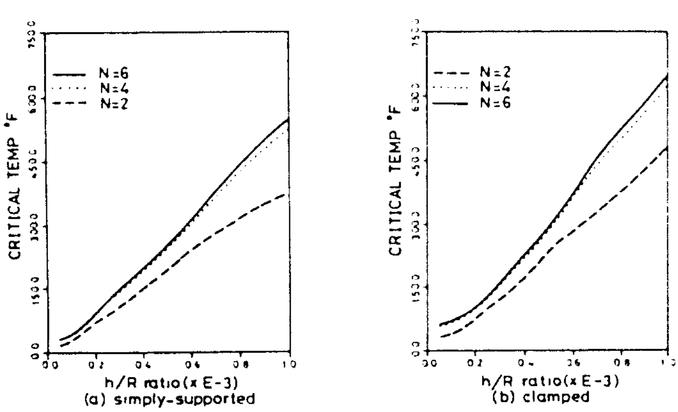

Fig. 3. Effect of radius of curvature R on critical temperature of thermal buckling. (a) Simply-supported. (b) Clamped. $E_1/E_0 = 21.0$, $E_2/E_0 = 1.7$, $E_3 = E_2$, $G_{12}/E_0 = 0.65$, $G_{23}/E_0 = 0.639$, $G_{13} = G_{12}$, $\nu_{12} = \nu_{13} = 0.21$, $\nu_{23} = 0.33$, $\alpha_{11} = -0.21$, $\alpha_{22}/\alpha_0 = \alpha_{33}/\alpha_0 = 16.0$, $E_0 = 1 \times 10^6$ psi, $\alpha_0 = 1 \times 10^{-6}$ in/in/°F.

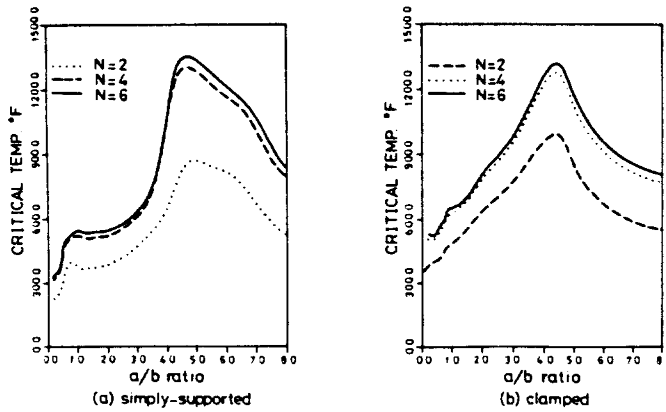

Fig. 4. Effect of aspect ratio a/b on critical temperature. (a) Simply-supported. (b) Clamped. $E_1/E_0 = 21.0$, $E_2/E_0 = 1.7$, $E_3 = E_2$, $G_{12}/E_0 = 0.65$, $G_{23}/E_0 = 0.639$, $G_{13} = G_{12}$, $\nu_{12} = \nu_{13} = 0.21$, $\nu_{23} = 0.33$, $\alpha_{11} = -0.21$, $\alpha_{22}/\alpha_0 = \alpha_{33}/\alpha_0 = 16.0$, $E_0 = 1 \times 10^6$ psi, $\alpha_0 = 1 \times 10^{-6}$ in/in/°F.

decrease the buckling temperature as compared to the case of the simply-supported boundaries. Thus as can be seen from the figure, there do exist values of h/R where the critical temperatures for both clamped and simply-supported boundaries are nearly the same.

(7) Critical temperature versus various ratios of E_1/E_2: Fig. 8a–c depicts the relationships of the critical temperatures versus ply angle under $E_1/E_2 = 3$, 10, and 50, respectively. As illustrated in this figure, the ply angle corresponding to the maximum critical temperature moves from about 30° to 45°; in addition, the mode interaction becomes more pronounced as E_1/E_2 increases.

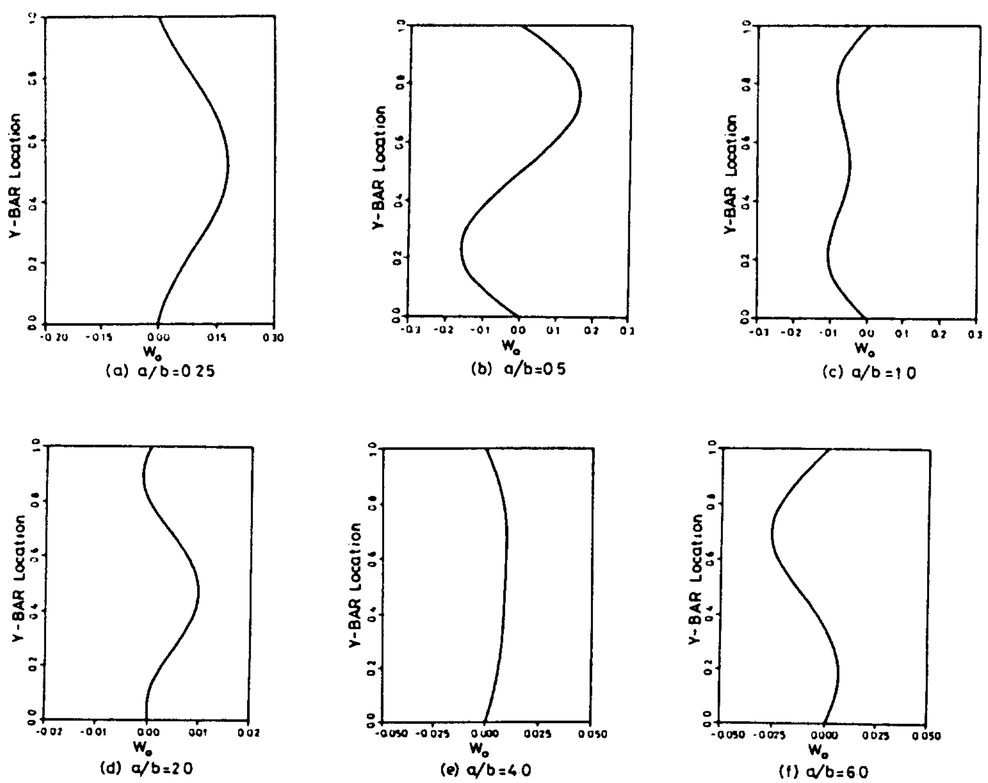

Fig. 5. Effect of various aspect ratios a/b on mode shape of thermal buckling for simply-supported edges at $\bar{x} = x/a = 0.5$ and various locations of $\bar{y} = y/b$. (a) $a/b = 0.25$; (b) $a/b = 0.5$; (c) $a/b = 1.0$; (d) $a/b = 2.0$; (e) $a/b = 3.0$; (f) $a/b = 6.0$.

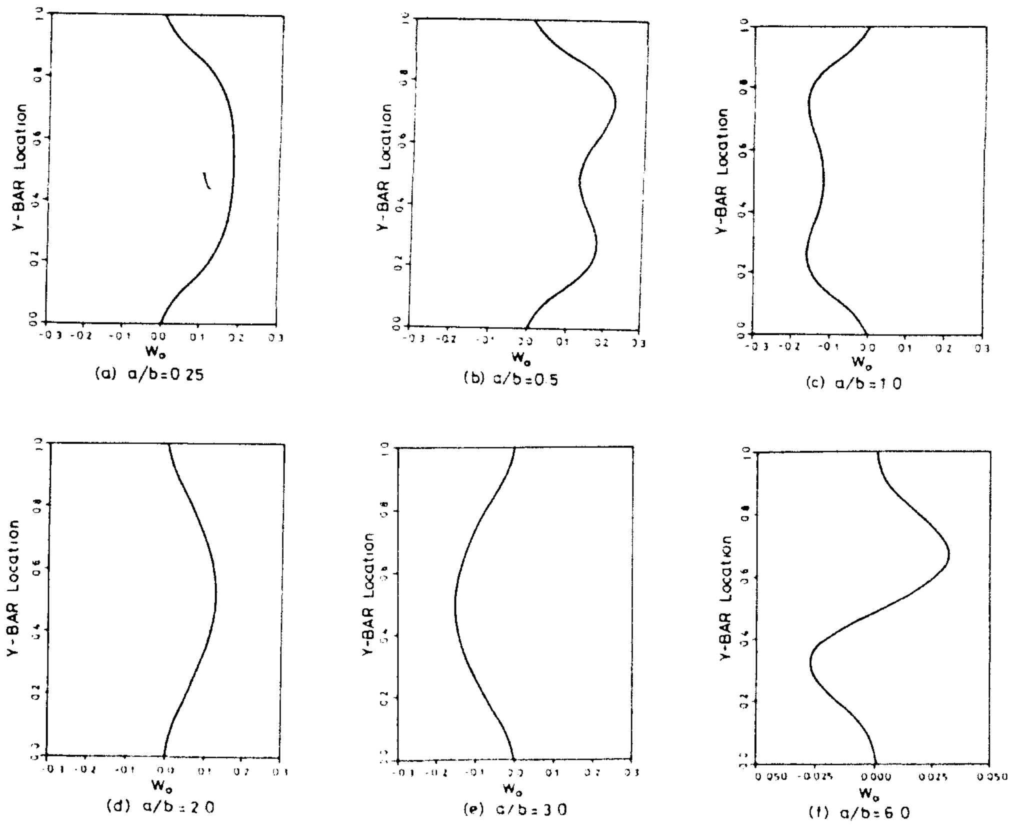

Fig. 6. Effect of various aspect ratios a/b on mode shape of thermal buckling for clamped edges at $\bar{x} = x/a = 0.5$ and various locations of $\bar{y} = y/b$. (a) $a/b = 0.25$; (b) $a/b = 0.5$; (c) $a/b = 1.0$; (d) $a/b = 2.0$; (e) $a/b = 3.0$; (f) $a/b = 6.0$.

CONCLUDING REMARKS

The thermal buckling of an antisymmetric angle ply laminated cylindrical shell panel subject to a uniform temperature field has been investigated. Appreciable errors may occur if a low order displacement field is used instead of a higher order one. Increase of curvature, number of layers with thickness fixed, and ratio of E_1/E_2 with E_2 fixed always raise the critical temperature of thermal buckling. As the ratio of E_1/E_2 varies from 3 to 50, the ply angle, where maximum critical temperature occurs, moves from near 30° to 45°. The ratio of the span a/b changes the buckling modes, which in turn affects the critical temperature, and such a phenomenon is more pronounced for the case of simply-supported boundaries

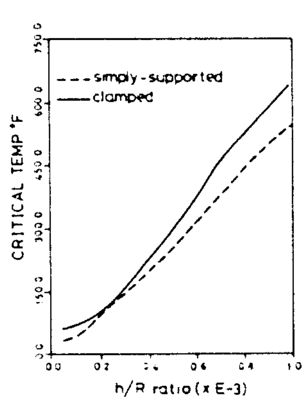

Fig. 7. Effect of boundary condition on critical temperature of thermal buckling.

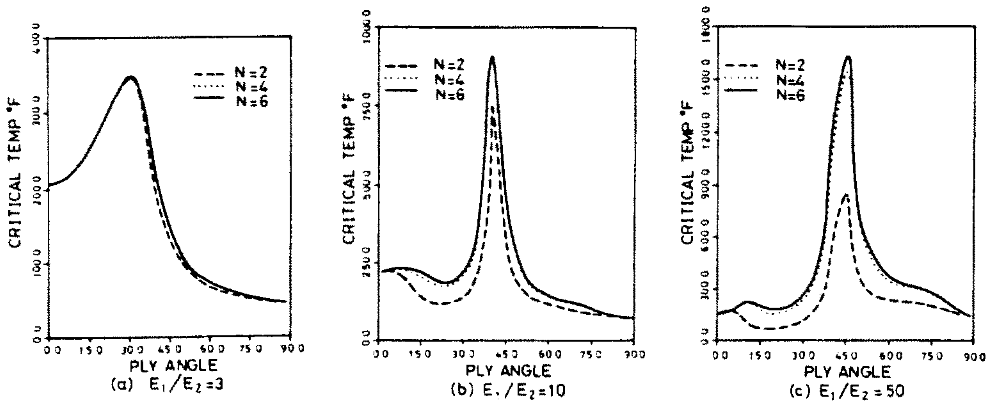

Fig. 8. Comparison of effect of modulus ratio E_1/E_2 on critical temperature of thermal buckling of the shell panel.

than clamped edges. Finally, although clamped boundaries increase the stiffness of the panel, compared to the simply-supported case, the thermal stresses are also raised, which tends to lower the critical temperature, such that in some cases the critical temperatures of the shell panel with clamped edges and simply-supported edges are nearly the same.

REFERENCES

Abir, D. and Nardo, S. V. (1959). Thermal buckling of circular cylindrical shell heated along an axial strip. *J. Aerospace Sci.* **26**, 803–808.

Brush, D. O. and Almroth, B. O. (1975). *Buckling of Bars, Plates, and Shells.* McGraw-Hill, New York.

Gupta, S. D. and Wang, I. C. (1973). Thermal buckling of orthotropical shells. *Fibre Sci. Technol.* **6**, 39–45.

Hoff, N. J. (1957). Buckling of thin cylindrical shell under hoop stress varying in axial direction. *J. Appl. Mech.* **24**, 405–412.

Hoff, J. N., Chao, C. C. and Madsen, W. A. (1964). Buckling of a thin-walled circular cylindrical shell heated along an axial strip. *J. Appl. Mech.* **31**, 253–258.

Novozhilov, V. V. (1953). *Foundations of Nonlinear Theory of Elasticity.* Graylock Press, New York.

Radhamohan, S. K. and Venkataramana, J. (1975). Thermal buckling of orthotropic cylindrical shells. *AIAA Jl* **13**, 397–399.

Ross, B., Mayers, J. and Jaworski A. (1965). Buckling of thin circular cylindrical shell heated along an axial strip. *Exp. Mech.* **6**, 247–256.

Ross, B., Hoff, N. J. and Horton, W. H. (1966). The buckling behavior of uniformly heated thin circular cylindrical shells. *Exp. Mech.* **6**, 529–537.

Stein, M. (1986) Nonlinear theory for plates and shells including the effects of transverse shearing. *AIAA Jl* **24**(9), 1537–1544.

Vinson, J. R. and Sierakowski, R. L. (1986). *The Behavior of Structures of Composite Materials.* Martinus Nijhoff, The Hague.

Washizu, K. (1986). *Variational Methods in Elasticity and Plasticity*, 3rd edn. Pergamon Press, Oxford.

Zuk, W. (1957). Thermal buckling of clamped cylindrical shells. *J. Aeronautical Sci.* **24**, 359.

Zukas, J. A. (1974). Effects of transverse normal and shear strains in orthotropic shells. *AIAA Jl* **12**, 1753–1756.